Wide-band electrical and electromechanical properties of polyvinylidene fluoride (PVDF) and polyvinylidene fluoride-trifluoroethylene (PVDF-TrFE) piezoelectric films using Electro-Acoustic Reflectometry

É. Maréchal, E. Géron, S. Holé

Wide-band electrical and electromechanical properties of polyvinylidene fluoride (PVDF) and polyvinylidene fluoride-trifluoroethylene (PVDF-TrFE) piezoelectric films using Electro-Acoustic Reflectometry

É. Maréchal, E. Géron, and S. Holé

Laboratoire de Physique et d'Étude des Matériaux (UMR8213),

CNRS – ESPCI Paris, PSL University – Sorbonne University, 10 rue Vauquelin, Paris, 75005, France[a]

(Dated: 1 April 2023)

Thin piezoelectric polymer films are used in more and more high frequency applications. However they are not well characterized up to the gigahertz range. In this paper, polyvinylidene fluoride (PVDF) and polyvinylidene fluoride-trifluoroethylene (PVDF-TrFE) films are mechanically and electrically characterized using the Electro-Acoustic Reflectometry (EAR) method from 20 MHz to 2 GHz. In addition to mechanical and electrical properties, nonuniform poling is detected in the tested PVDF-TrFE samples showing a larger piezoelectric constant in the middle of the film and thus generating both even and odd resonance modes.

[a]stephane.hole@espci.fr

Keywords: Piezoelectric polymer films; dielectric properties; electromechanical properties; Electro-Acoustic Reflectometry (EAR).

I. INTRODUCTION

Piezoelectric materials have found applications in numerous areas. Since their discovery[1] polarized polyvinylidene fluoride (PVDF) polymer films have shown good piezoelectric properties that can provide an alternative to piezoelectric crystals: polymers are indeed flexible, can be made very thin, are soft, have a low thermal conductivity, and are generally low cost. In addition, they can be easily patterned to form complex shapes covering large areas. Their softness makes them particularly well suited to be coupled with fluids since their acoustic impedance is comparable to that of water. They have found many applications in sensors and photonics, and their use is compatible with microelectronics[2–5]. Piezoelectric films in the micrometer thickness range correspond to higher frequency applications (up to the gigahertz range), that are now reachable at moderate cost with the progress of high frequency electronic devices. The characterization of the full properties (electrical, mechanical, uniformity) of these piezoelectric films, particularly at very high frequency, is therefore of interest.

When synthesized, PVDF polymer films are not polarized (nor piezoelectric): permanent polarization and piezoelectricity is achieved with different methods that consist in aligning the polar molecules in the same direction[1]. The standard method to permanently polarize the films, known as poling method, consists in applying a static electric field as high as about 300 kV/mm along the film thickness when the polymer is heated to about 100°C. Before poling, the films generally have been initially stretched to several times of their initial size at a slightly higher temperature, up to 150°C. After poling, a slow cooling down

to room temperature in the presence of the electric field prepares the film with a uniform dipole distribution through the film thickness responsible for piezoelectricity. For rather thick films (larger than 100 μm), the growing of the poling process was studied using the Pressure-Wave-Propagation Method (PWP)[6]. So far, it has not been tested for thinner samples owing to the lack of appropriate measurement method.

Recently, a measurement method called the Electro-Acoustic Reflectometry (EAR) has been proposed to break the limit of spatial resolution and reach the sub-micrometer range for the space charge distributions in dielectric films[7]. The EAR method is based on the measurement of the electro-elastic coupling in the material due to an electrical excitation swept over a very large frequency range. The electro-elastic coupling at each excitation frequency is extracted from the electrical impedance of the sample. Finally, from the variation of the electro-elastic coupling as a function of frequency, the charge distribution is recovered by an inverse Fourier transform. This method is particularly relevant for the characterization of thin piezoelectric films since the signal is proportional to $\partial e_{33}/\partial x_3$ through the film thickness axis x_3 where e_{33} is the piezoelectric stress coefficient expressed in Coulombs per square meter.

The EAR method is applied in this paper to piezoelectric polymer films of PVDF and PVDF-TrFE (polyvinylidene fluoride-trifluoroethylene). The measurement results of the electromechanical and electrical properties of PVDF films with three different thicknesses from 3 to 9 μm are given, as well as their equivalent charge distribution along the thickness axis. The principle of the EAR method is first briefly described and details are given on the experimental set-up and the samples. Experimental results are presented and interpreted

in the light of known models. Then, the method used to isolate the electrical contributions (permittivity and electric losses) and the mechanical contributions (coupling factor and mechanical losses) from the electrical measurement is explained. Finally, results and equivalent charge distributions are presented and discussed before drawing conclusions.

II. EAR METHOD, SET-UP AND SAMPLES

A. EAR principle

Nondestructive direct space charge distribution measurement methods use the same principle: the sample under test is perturbed from its electro-elastic equilibrium and thus generates a measurable signal when returning to equilibrium[8]. The perturbation can be initiated by a thermal excitation (thermal method)[9], an elastic excitation (pressure-wave-propagation method or PWP)[10] or an electrical excitation (pulsed-electro-acoustic method or PEA)[11]. Though thermal diffusion is a slow process and thus allows high spatial resolution to be reached, the thermal method suffers from the evolution of the temperature profile during the diffusion, which makes it difficult to recover the space charge distribution from measurements. The inverse calculation to recover the space charge distribution is indeed an ill-posed problem, hence noise may have a very large impact on the result reducing confidence in the calculation. Concerning PWP and PEA methods, their implementation requires transfer of elastic waves through at least one interface of the material under test to either excite it (PWP) or obtain the signal (PEA). Therefore the mechanical conditions at the interfaces

and the spatial dispersion of any material defects make high spatial resolution difficult to reach.

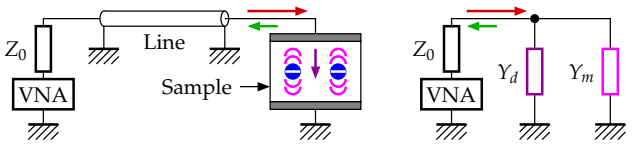

FIG. 1. (left) Sketch of the measurement setup. (right) Equivalent circuit. A Vector Network Analyzer (VNA) excites the sample (red arrows) at successive frequencies over a broad range through a line of impedance Z_0. Electric reflections from the sample (green arrows) depend on its dielectric properties (dark magenta) and elastic waves generated by the charges (light magenta). This is equivalent to a dielectric admittance Y_d in parallel with a mechanical admittance Y_m.

The EAR method (Electro-Acoustic Reflectometry) has been introduced to overcome these problems[12,13]. This method is also based on the perturbation of the electro-elastic equilibrium. The sample is electrically excited at successive frequencies distributed over a broad frequency range (see Figure 1, red arrows). At each of these frequencies, the sample consumes one part of the excitation energy (see Figure 1 in dark and light magenta) and reflects back the other part (see Figure 1, green arrows). As the reflected part is the complement of the consumed part, the measurement of the reflected part is an indirect way of measuring the sample consumption. A large fraction of the consumed energy depends on the dielectric properties of the sample and can be seen as an admittance Y_d (See Figure 1 in dark magenta). A smaller fraction depends on the elastic waves generated by charges due to the electrical excitation and can be seen as an additional electrical admittance Y_m in parallel (see Figure 1 in light magenta). Thanks to mechanical resonances in the sample under test,

the reflected energy due to elastic waves appears in the signal as notches localized at given frequencies whereas the reflected energy due to dielectric properties evolves smoothly over the whole bandwidth. This makes it possible to isolate the reflected energy due to elastic waves from the one due to dielectric properties and thus to calculate independently the mechanical admittance Y_m and the dielectric impedance Y_d. As a consequence, information on both mechanical and dielectric properties of the sample are obtained. In addition, a reconstruction of the impulse response using the reflected energy due to elastic waves and an inverse Fourier transform allows a signal similar to the space charge distribution to be recovered as in the case of the PWP or PEA methods, space and time being connected by the velocity of sound. One advantage of the EAR method is that higher frequencies (so better spatial resolution) can be reached because excitation and measurement are directly made inside the sample (no interface to cross).

B. EAR set-up

The experimental set-up is pictured in Figure 2. At very high frequencies, propagation effects are no longer negligible and the use of a Vector Network Analyzer (VNA) with its probe station is the standard way to control and measure with great accuracy electrical reflections from the samples[14]. In this study, a ZNB40 VNA from Rohde&Schwarz and a station equipped with ACP RF probe from FormFactor were used to measure S_{11}, which is the electrical reflection coefficient from the sample under test. The whole set-up is calibrated by the Open-Short-Match procedure before measurements[15] using 106-683 calibration kit from FormFactor. This standard and precise calibration procedure allows losses and phasing

to be compensated at all frequencies caused by the propagation in cables and probe, and ensures that measured S_{11} is the response of the sample only. The RF probe has 1-mm pitch and 10-GHz bandwidth. The probe station is equipped with a binocular microscope and a 3-axis micrometer displacement stage to precisely place the probe signal tip on the sample and the other probe tips on the ground plane (See inset in Figure 2).

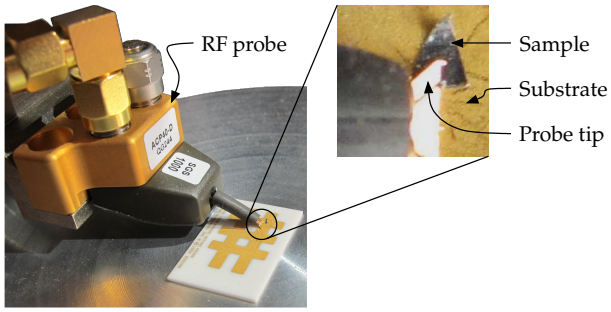

FIG. 2. The VNA is connected to an RF probe whose signal tip is in contact to one of the sample electrodes, the others being connected to ground through a golden substrate. The inset shows a larger view of the sample at the probe tip.

C. Samples and procedure

All piezoelectric samples are uni-axially oriented along the thickness axis. PVDF samples were purchased from Solvay company. From the data-sheet, they are made of polycristalline PVDF polymer with crystalline domains in the β-phase[16,17]. They are 9-μm thick and aluminum coated on both sides. PVDF-TrFE samples were purchased from PolyK company. From the data-sheet, this is a copolymerisation with 75% VDF and 25% TrFE. They are 5-μm and 3-μm thick and gold coated on both sides. All samples have a typical area of

slightly less than 1 mm^2. Their exact surface was determined from images for geometrical factor compensation purposes.

Samples were placed on a commercial contact substrate covered with a highly conductive golden copper plane that acted as ground plane. The measurements were carried out over a bandwidth ranging from 20 MHz to 2.5 GHz with 500 kHz resolution.

III. EXPERIMENTAL RESULTS

A. Measurements

The typical spectra showing the reflection coefficient amplitude $|S_{11}|$ are presented for the 3 sample types in Figure 3. All $|S_{11}|$ spectra show a base line varying slowly with frequency, which corresponds to the dielectric response (permittivity and electrical losses) of the material, on which various peaks appear. These peaks correspond to the additional energy consumption resulting from the mechanical resonances due to the electro-elastic coupling. The first resonance occurs at about 129 MHz for the 9-μm thick PVDF sample, 198 MHz for the 5-μm thick PVDF-TrFE sample and 333 MHz for the 3-μm thick PVDF-TrFE sample. Due to symmetrical reasons and considering a uniform sample, the higher order resonances correspond more or less to odd multiples of the fundamental frequency[13]. For PVDF-TrFE samples however, some elastic resonances can be detected at even harmonics (see dotted circles in Figure 3). This is an indication of a nonuniform material. Though mechanical nonuniformities could generate resonances at even harmonics by themselves, they would have a significant amplitude only if the mechanical nonuniformities were quite large thus

producing big mechanical mismatches. For apparent mechanically uniform materials, such as those of the samples described in this paper, even harmonics are much more probably produced by a nonuniform poling. This indeed breaks the sample symmetry, generating in turn detectable even harmonics even for quite small nonuniform poling.

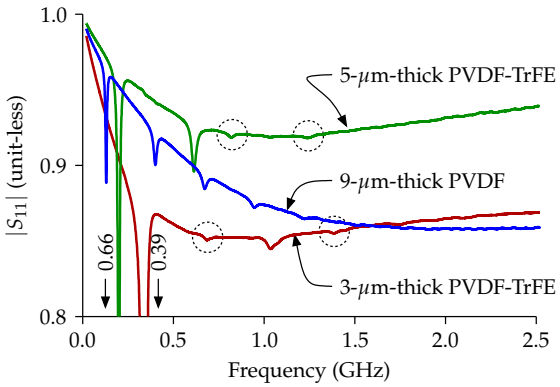

FIG. 3. Typical $|S_{11}|$ measurement results for piezoelectric samples with different thicknesses. Only odd harmonics are detected with PVDF whereas odd and even harmonics (inside dotted circles) are present with PVDF-TrFE.

As electrical and mechanical responses can be seen as two impedances in parallel (see Figure 1, right), it is preferable to study the sample admittance $Y(\omega)$ as a function of circular frequency ω instead of $S_{11}(\omega)$ directly obtained from raw measurements. One has

$$Y(\omega) = Y_0 \times \frac{1 - S_{11}(\omega)}{1 + S_{11}(\omega)}, \tag{1}$$

where $Y_0 = 0.02\,\mathrm{S} = 1/(50\,\Omega)$ is the admittance of the VNA port.

Figure 4 presents the typical admittance for the 3 kinds of samples corrected from their geometrical factor, *i.e.* multiplied by thickness over area. This corresponds to an equivalent conductivity. The imaginary part is much larger than the real part and well proportional to

frequency which corresponds globally to a capacitive behavior. The real part corresponds to the losses in the material. The mechanical resonances are visible and can be grossly modeled by a series of RLC circuits (motion branches) in parallel with a capacitor (static branch) as in the Butterworth Van Dyke electrical model[18,19].

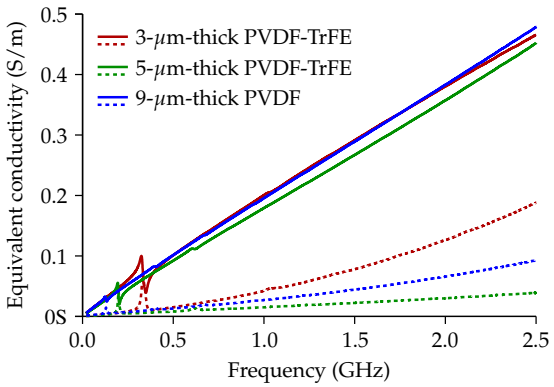

FIG. 4. Typical imaginary part (solid lines) and real part (dashed lines) of the admittance of the different kinds of samples corrected from their geometrical factor (equivalent conductivity). As expected a capacitive behavior is obtained on which resonances are visible.

B. Uniform material model

With thin samples compared to their diameter, elastic resonances originate only from the thickness extension mode of vibration (TE mode). The admittance at resonance is a standard way to extract the electro-mechanical properties of the material for the corresponding mode of excitation, a method known as resonance method[20]. In the case of a uniform loss-less piezoelectric material under free surface conditions, the admittance Y for the TE mode is

given by[21]:

$$Y(\omega) = \underbrace{\jmath\omega C_0}_{Y_d} + \underbrace{\frac{\jmath\omega C_0 k_{33}^2}{\frac{\omega d}{2v_s}\cot(\frac{\omega d}{2v_s}) - k_{33}^2}}_{Y_m} \tag{2}$$

where $\jmath^2 = -1$, C_0 is the sample capacitance and d the sample thickness. The sample capacitance is simply related to the permittivity at constant strain ϵ_{33}^S by $C_0 = \epsilon_{33}^S A/d$ where A is the sample area. Sound velocity v_s is related to the elastic stiffness coefficient at constant electric displacement field c_{33}^D with the standard relation $v_s^2 = c_{33}^D/m_v$, where m_v is the mass density. The coupling factor k_{33} is defined as the square root of the ratio between stored and brought energies such that $k_{33}^2 = e_{33}^2/(\epsilon_{33}^S c_{33}^D)$[22].

Equation (2) has two clearly identified terms: the first one corresponds to the static capacitance (dielectric admittance Y_d), and the second one corresponds to the different mechanical resonances of odd orders (mechanical admittance Y_m). Since the Y_m is proportional to Y_d, the impedance $Z = 1/Y$ has also a convenient expression:

$$Z(\omega) = \frac{1}{\jmath\omega C_0} \times \left(1 - k_{33}^2 \frac{\tan(\frac{\omega d}{2v_s})}{\frac{\omega d}{2v_s}}\right). \tag{3}$$

Dielectric and elastic losses can be respectively introduced through the loss tangent $\tan\delta_d$ in the permittivity and the loss tangent $\tan\delta_m$ in the elastic compliance so that

$$\epsilon^S \to \epsilon^S(1 - \jmath\tan\delta_d) \quad \text{and} \quad c_{33}^D \to \frac{c_{33}^D}{1 - \jmath\tan\delta_m}. \tag{4}$$

In the same way, the coupling factor experiences both kind of losses and becomes

$$k_{33}^2 \to k_{33}^2(1 - \jmath\tan\delta_d)(1 - \jmath\tan\delta_m). \tag{5}$$

The complex admittance and impedance for a piezoelectric material with losses can then be rewritten respectively as[23]

$$Y(\omega) = \jmath\omega C_0\,(1-\jmath\tan\delta_d) + \frac{\jmath\omega C_0\,(1-\jmath\tan\delta_d)^2\,k_{33}^2}{\frac{\jmath\omega d}{2v_s}\,(1+\jmath\frac{\tan\delta_m}{2})\,\coth(\frac{\jmath\omega d}{2v_s}\,(1-\jmath\frac{\tan\delta_m}{2})) - k_{33}^2\,(1-\jmath\tan\delta_d)}, \quad (6)$$

$$Z(\omega) = \frac{1}{\jmath\omega C_0\,(1-\jmath\tan\delta_d)} - \frac{k_{33}^2}{\jmath\omega C_0}\,\frac{\tanh(\frac{\jmath\omega d}{2v_s}\,(1-\jmath\frac{\tan\delta_m}{2}))}{\frac{\jmath\omega d}{2v_s}\,(1+\jmath\frac{\tan\delta_m}{2})}. \quad (7)$$

As shown in[23,24], the mechanical coupling factor k_{33}, the piezoelectric stress constant e_{33} and the mechanical loss tangent $\tan\delta_m$ can be measured at first resonance frequency. Therefore, the study of higher resonance orders allows the elastic properties to be to accessed on a broader spectrum range. In addition, by measuring the capacitance and the electrical losses on the nonresonant part of the spectrum, the dielectric constant and the electrical losses can be determined, knowing the sample geometrical factor.

Equations (6) and (7) describe very well the measurements insofar as the piezoelectric material is uniform and its dielectric constant, losses and coupling factor have a sufficiently slow evolution over the whole spectrum range. However, when the piezoelectric material is no longer uniform, Expressions (6) and (7) can no longer directly be used.

C. Measurement analysis

In the case of actual measurements, at least for PVDF-TrFE samples, even harmonics are present so (6) and (7) do not directly apply. With mechanical resonances showing localized fast spectrum variations compared to dielectric behavior, it is relatively easy to isolate the dielectric behavior from the measurements and thus extract C_0 and $\tan\delta_d$ from the base

line. Once done, these terms can be combined together with the impedance which leads, supposing a uniform material, to

$$\frac{1}{1-\jmath\tan\delta_d} - \jmath\omega C_0 Z(\omega) = k_{33}^2 \frac{\tanh(\frac{\jmath\omega d}{2v_s}(1-\jmath\frac{\tan\delta_m}{2}))}{\frac{\jmath\omega d}{2v_s}(1+\jmath\frac{\tan\delta_m}{2})}. \tag{8}$$

It is possible to decompose the second member of (8) as the sum of Lorentzian functions since

$$\frac{\tanh(\jmath w(1-\jmath\zeta))}{\jmath w(1+\jmath\zeta)} = \frac{1}{1+\zeta^2}\sum_{k=0}^{\infty}\frac{2}{\left(\frac{k\pi+\pi/2}{1-\jmath\zeta}\right)^2 - w^2}, \tag{9}$$

where w is a reduced circular frequency, here $w \equiv \frac{\omega d}{2v_s}$, and ζ is a loss factor, here $\zeta \equiv \frac{\tan\delta_m}{2}$. As a consequence, each maximum in (8) can be reasonably assumed associated with a single normalized Lorentzian function $L(w)$, defined as

$$L(w) = \frac{2\jmath\alpha w_R^2}{w_R^2 + 2\jmath\alpha w_R^2 - w^2}, \tag{10}$$

with

$$\begin{cases} w_R = \dfrac{\sqrt{1-\zeta^2}}{1+\zeta^2} \times (k\pi + \pi/2) \\ \alpha = \dfrac{\zeta}{1-\zeta^2} \end{cases} \tag{11}$$

since (9) can be rewritten as

$$\frac{\tanh(\jmath w(1-\jmath\zeta))}{\jmath w(1+\jmath\zeta)} = \frac{1}{1+\zeta^2}\sum_{k=0}^{\infty}\frac{L(w)}{\jmath\alpha w_R^2}. \tag{12}$$

The natural circular frequency w_R allows v_s to be determined and damping factor α allows $\tan\delta_m$ to be determined. The square of the coupling coefficient k_{33}^2 is directly obtained from the magnitude of the normalized Lorentzian function peak multiplied by $(1+\zeta^2)\,\alpha w_R^2$. This is pushed further to nonuniform materials in the following subsections.

1. *Dielectric properties*

Figure 5 shows the relative permittivity and $\tan\delta_d$ as a function of frequency. This information is obtained from the admittance taking into account geometrical factors and canceling resonances by appropriate Lorentzian functions. As a small residual may remain in the cancellation (see inset in Figure 5), a smoothing is applied. It consists in replacing by a spline function the part of the curve that includes the residual.

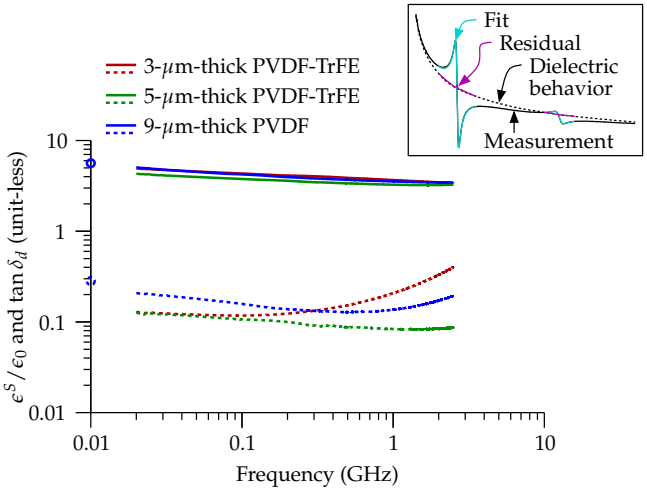

FIG. 5. Typical relative permittivity ϵ^S/ϵ_0 (solid lines) and dielectric losses $\tan\delta_d$ (dashed lines) of the different kinds of samples. The circles on the y-axis correspond to the higher frequency values obtained from[25]. In the inset, mechanical resonance fits on a measurement and residual smoothing to obtain the material dielectric behavior.

Relative permittivity ϵ^S/ϵ_0, where ϵ_0 is the vacuum permittivity, reduces regularly on the frequency range from about 5 to about 3.5. Losses experience similar trend at low frequency but increase rapidly at higher frequency. PVDF has a higher $\tan\delta_d$ than PVDF-TrFE at low frequency (60% larger). Compared to 5-μm-thick PVDF-TrFE, the cutoff frequency of

9-μm-thick PVDF is much lower, slightly under 1 GHz. The comparison of PVDF-TrFE samples shows a rapid increase of losses for the thinner sample, probably due to the film processing which may be less efficient in the case of thinner materials. This is also visible in the relative permittivity since the one of the 5-μm-thick sample is 15% lower.

All the measurements are consistent with the ones reported in[23,24] using resonant methods. The measured relative permittivity at high frequency is much lower than the one at very low frequency (dc value) since a value between 10 and 13 is generally reported for β-PVDF. For instance in[25] the evolution of relative permittivty and $\tan\delta_d$ was measured between 100 Hz and 10 MHz for PVDF films with different crystalline properties. Relative permittivity reaches 13 for β-PVDF below 100 kHz and decreases monotonically to 5 at 10 MHz. Concerning $\tan\delta_d$, it starts from 0.03 at 100 Hz and reaches as high as 0.3 around 2.5 MHz and begins to decrease slowly above. This is consistent with the transition of relative permittivity around 1 MHz[26] and the decrease continues reaching about 0.13 at 500 MHz.

The increase of $\tan\delta_d$ at higher frequency can be attributed to another effect since no relative permittivity variation is observed. The contact resistance at the electrodes can indeed enter into consideration. The same applies to the 3-μm-thick PVDF-TrFE sample.

The general behavior of relative permittivity and $\tan\delta_d$ as a function of frequency is well described by Xia and Zhu[5,26]. The observed variations at low frequencies correspond to different polarization processes in polymers that are too slow to contribute at higher frequencies. Therefore, in sub-gigahertz and gigahertz ranges, the relative permittivity and $\tan\delta_d$ decrease with frequency.

2. *Electro-mechanical properties*

Using the combination in the left member of (8), Lorentzian functions (10) can be fitted on each resonance. Results are reported and interpreted for each material in tables I, II and III. Velocity v_s, mechanical loss $\tan\delta_m$ and coupling coefficient k_{33} are obtained from

$$\begin{cases} v_s = \dfrac{2df_R}{N}\,\dfrac{1+\zeta^2}{\sqrt{1-\zeta^2}} \\ \tan\delta_m = 2\zeta \\ k_{33} = \dfrac{2}{\pi N}\sqrt{M\zeta\,\dfrac{1+\zeta^2}{1-\zeta^2}} \end{cases} \tag{13}$$

where f_R is the resonance frequency of the harmonic of order N, and M is the magnitude of the Lorentzian (10) to fit the resonance.

Velocity does not significantly vary with frequency, being about 2420 m/s for PVDF and 2050 m/s for PVDF-TrFE. Mechanical losses $\tan\delta_m$ are quite similar for all materials, typically $\tan\delta_m = 0.05$, slightly better for the 5-μm-thick PVDF-TrFE than other samples, emphasizing further a better process control for this material thickness. The coupling coefficient is much larger for PVDF-TrFE (about 0.25, which corresponds to the manufacturer value) than for PVDF (0.166, which is close to the standard value for β-PVDF[23,24]). However k_{33} decreases more rapidly with PVDF-TrFE than with PVDF. For high harmonic orders, PVDF has therefore a better coupling. This variation of the coupling coefficient has already been reported in[27] for piezoelectric thin films resonators made of aluminum nitride (AlN) and lead zirconate titanate (PZT). Early studies on PVDF[28] on a much narrower frequency range have also reported the slight decreasing of k_{33} as a function of frequency.

TABLE I. (upper part) Lorentzian parameters (resonance frequency f_R, loss factor ζ and magnitude M) for the 9-μm-thick PVDF sample and (lower part) deduced mechanical characteristics (sound speed v_s, mechanical losses $\tan\delta_m$ and coupling coefficient k_{33}) for each detectable harmonic order. Unit-less when not specified.

Order N	1st	3rd	5th	7th	9th
f_R (MHz)	131.0	400.5	671.5	945.0	1224.0
ζ	0.0339	0.0257	0.0240	0.0219	0.0204
M	0.3307	0.0407	0.0141	0.0058	0.0025
v_s (m/s)	2362	2405	2419	2432	2450
$\tan\delta_m$	0.0678	0.0514	0.0480	0.0438	0.0408
k_{33}	0.166	0.152	0.145	0.124	0.100

3. Equivalent charge distribution

Equivalent charge distribution corresponds to the opposite of the divergence of the dipole distribution for piezoelectric materials. In the case of uniform piezoelectric materials, equivalent charges appear only at the sample boundaries, positive on one side and negative on the other side. In the case of a nonuniform piezoelectric material, additional equivalent charges appear inside the sample, that is to say between the charges at the boundaries.

The equivalent charge distribution can be well estimated with the EAR method from the inverse Fourier transform of the mechanical resonances which are characterized by the

TABLE II. (upper part) Lorentzian parameters (resonance frequency f_R, loss factor ζ and magnitude M) for the 5-μm-thick PVDF-TrFE sample and (lower part) deduced mechanical characteristics (sound speed v_s, mechanical losses $\tan\delta_m$ and coupling coefficient k_{33}) for each detectable harmonic order. Unit-less when not specified.

Order N	1st	3rd	4th	5th	6th
f_R (MHz)	203.0	612.0	813.5	1010.0	1237.5
ζ	0.0240	0.0240	0.0282	0.0355	0.0245
M	0.9171	0.0413	0.0036	0.0018	0.0024
v_s (m/s)	2032	2042	2036	2024	2064
$\tan\delta_m$	0.0480	0.0480	0.0564	0.0710	0.0491
k_{33}	0.233	0.148	0.063	0.063	0.072

set of Lorentzian functions described in Section III C[13]. Since the lateral dimensions of the samples are much larger compared to their thickness, the plane wave approximation applies and the time axis in the inverse Fourier transformation (impulse response) is comparable to the position in depth knowing the velocity of sound. Figure 6 shows such inverse Fourier transformations for the three kinds of samples. Zero padding is used to obtain a sufficient time resolution.

For the 9-μm-thick PVDF sample, the equivalent charges are well localized at the sample boundaries, *i.e.* no significant equivalent charge is detected inside the sample. This corresponds to a uniformly poled material because the changes in piezoelectric coefficient

TABLE III. (upper part) Lorentzian parameters (resonance frequency f_R, loss factor ζ and magnitude M) for the 3-μm-thick PVDF-TrFE sample and (lower part) deduced mechanical characteristics (sound speed v_s, mechanical losses $\tan\delta_m$ and coupling coefficient k_{33}) for each detectable harmonic order. Unit-less when not specified.

Order N	1st	2nd	3rd	4th	5th
f_R (MHz)	346.5	674.5	1025.5	1387.5	1747.5
ζ	0.0309	0.0417	0.0245	0.0178	0.0427
M	0.8646	0.0051	0.0113	0.0031	0.0057
v_s (m/s)	2082	2029	2053	2082	2103
$\tan\delta_m$	0.0618	0.0834	0.0491	0.0356	0.0853
k_{33}	0.257	0.046	0.078	0.047	0.123

between the inside and the outside of the sample are well localized at the sample boundaries. However, for both PVDF-TrFE samples, equivalent charges are clearly detected inside the material, as shown in the dotted circles in Figure 6. This indicates that e_{33} is larger in the middle of the sample than at its boundaries since the piezoelectric coefficient changes are more progressive. This result confirms the assumption raised from the detection of even harmonics, already detected in the S_{11} spectra shown in Figure 3, and gives in addition the location of these nonuniformities.

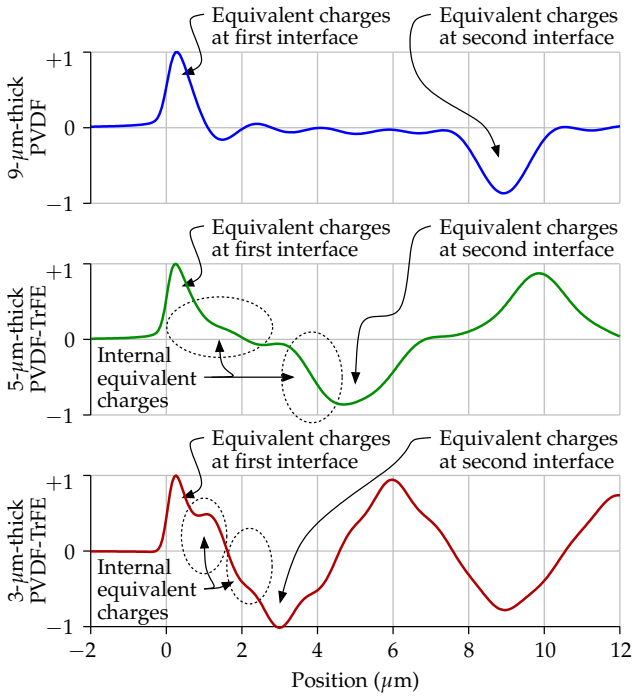

FIG. 6. Equivalent charge distribution for the different samples as a function of position: PVDF 9μm-thick (blue), PVDF-TrFE 5 and 3 μm-thick (green and red). A uniform material presents only opposite equivalent charges at the material boundaries (indicated here as first and second interfaces). This is actually the case for the PVDF sample but not for both PVDF-TrFE samples which present additional equivalent charges inside the material (dotted circles) indicating a variation of the piezoelectric coefficient as a function of depth.

IV. CONCLUSION

In this work, dielectric and electromechanical properties of PVDF and PVDF-TrFE piezoelectric materials have been determined over a very broad frequency range, up to above the gigahertz. This extends above 10 MHz already reported results.

The Electro-Acoustic-Reflectometry (EAR) method has been used for all measurements. Information was extracted from measurements by fitting mechanical resonances with ap-

propriate Lorentzian functions. This makes the distinction of dielectric and mechanical responses possible and thus the extraction of dielectric and mechanical properties of the tested piezoelectric film. In addition the film poling uniformity can be obtained.

It is found that tested PVDF-TrFE samples are not uniformly poled compared to PVDF. Their piezoelectric coefficient is actually found larger in the middle of the material which generates even modes of resonance when excited. In addition, the conductivity of electrodes seems to impact the material efficiency at higher frequency.

REFERENCES

[1]H. Kawai, "The piezoelectricity of poly (vinylidene fluoride)," Japanese Journal of Applied Physics **8**, 975–976 (1969) doi: 10.1143/JJAP.8.975.

[2]J. Victor Chatigny and L. Robb, "Sensors: making the most of piezo film," Sensor Review **7**, 15–20 (1987) doi: 10.1108/eb007709.

[3]G. Harsanyi, *Polymer films in sensor applications* (Lancaster, PA, 1995) (1995) iSBN: 9781566762014.

[4]G. Harsanyi, "Polymer films in sensor applications: a review of present uses and future possibilities," Sensor Review **20**, 98–105 (2000) doi: 10.1108/02602280010319169.

[5]W. Xia and Z. Zhang, "PVDF-based dielectric polymers and their applications in electronic materials," IET Nanodielectrics **1**, 17–31 (2018) doi: 10.1049/iet-nde.2018.0001.

[6]C. Laburthe Tolra, C. Alquié, and J. Lewiner, "Polarization of VDF-TrFE copolymer films at elevated temperature," IEEE Transactions on Electrical Insulation **28**, 344–348 (1993)

303 doi: 10.1109/14.236213.

304 [7]L. Hamidouche, E. Géron, T. Ditchi, and S. Holé, "High Frequency Spectroscopy for High
305 Spatial Resolution Space Charge Measurements," in *2014 IEEE International Symposium*
306 *on Electrets (ISE)*, Baltimore, USA (2014), p. IX.8.

307 [8]S. Holé, T. Ditchi, and J. Lewiner, "Non-destructive methods for space charge distribution
308 measurements: what are the differences?," IEEE Transactions on Dielectrics and Electrical
309 Insulation **10**, 670–677 (2003) doi: 10.1109/TDEI.2003.1219652.

310 [9]R. Collins, "Analysis of spatial distribution of charges and dipoles in electrets by a
311 transient heating technique," Journal of Applied Physics **47**, 4804–4808 (1976) doi:
312 10.1063/1.322521.

313 [10]P. Laurençeau, G. Dreyfus, and J. Lewiner, "New principle for the determination of po-
314 tential distributions in dielectrics," Phys. Rev. Lett. **38**, 46–49 (1977) doi: 10.1103/Phys-
315 RevLett.38.46.

316 [11]T. Maeno, H. Kushibe, T. Takada, and C. M. Cooke, "Pulsed electro-acoustic method
317 for the measurement of volume charges in e-beam irradiated PMMA," in *Conference on*
318 *Electrical Insulation Dielectric Phenomena - Annual Report 1985* (1985), pp. 389–397, doi:
319 10.1109/CEIDP.1985.7728298.

320 [12]L. Hamidouche, E. Géron, and S. Holé, "Very high spatial resolution space charge measure-
321 ment using electro-acoustic reflectometry (EAR)," IEEE Electrical Insulation Magazine
322 **33**, 9–16 (2017) doi: 10.1109/MEI.2017.8014386.

[13]L. Hamidouche, E. Géron, and S. Holé, "Physical investigation of the Electro-Acoustic-Reflectometry method for space charge measurements," Physica Scripta **94**, 115006 (2019) doi: 10.1088/1402-4896/ab2105.

[14]D. Pozar, *Microwave Engineering*, Vol. 4th ed. , John Wiley & Sons, New York (2011).

[15]"R&S®ZNB/ZNBT User Manual" https://scdn.rohde-schwarz.com/ ur/ pws/ dl_downloads/ pdm/ cl_manuals/ user_manual/ 1173_9163_01/ ZNB_ZNBT_UserManual_en_63.pdf, consulted on March 28, 2023.

[16]M. Broadhurst, G. Davis, J. McKinney, and R. Collins, "Piezoelectricity and pyroelectricity in polyvinylidene fluoride, a model," Journal of Applied Physics **49**, 4992–4997 (1978) doi: 10.1063/1.324445.

[17]G. Sessler, "Piezoelectricity in polyvinylidenefluoride," The Journal of the Acoustical Society of America **70**, 1596–1608 (1981) doi: 10.1121/1.387225.

[18]S. Butterworth, "On electrically-maintained vibrations," Proceedings of the Physical Society of London **27**, 410–424 (1914) doi: 10.1088/1478-7814/27/1/330.

[19]K. Van Dyke, "The electrical networl equivalent of a piezo-electric resonator," in *Minutes of the Washington Meeting, April 24 and 25, 1925*, American Physical Society (1925), Vol. 25, p. 895, doi: 10.1103/PhysRev.25.880.

[20]"IEEE Standard on Piezoelectricity," ANSI/IEEE Std 176-1987 (1988) doi: 10.1109/IEEESTD.1988.79638.

[21]T. Meeker, "Thickness mode piezoelectric transducers," Ultrasonics **10**, 26–36 (1972) doi: 10.1016/0041-624X(72)90210-7.

[22]W. Mason, *Piezoelectric crystals and their application to ultrasonics.*, The Bell Telephone Laboratories series (Van Nostrand, New York, 1950).

[23]K. Koga and H. Ohigashi, "Piezoelectricity and related properties of vinylidene fluoride and trifluoroethylene copolymers," Journal of Applied Physics **59**, 2142–2150 (1986) doi: 10.1063/1.336351.

[24]H. Ohigashi, "Electromechanical properties of polarized polyvinylidene fluoride films as studied by the piezoelectric resonance method," Journal of Applied Physics **47**, 949–955 (1976) doi: 10.1063/1.322685.

[25]J. Li, M. Qingjie, W. Li, and Z. Zhang, "Influence of Crystalline Properties on the Dielectric and Energy Storage Properties of Poly(vinylidene fluoride)," Journal of Applied Polymer Science **122**, 1659–1668 (2011) doi: 10.1002/app.34020.

[26]L. Zhu, "Exploring strategies for high dielectric constant and low loss polymer dielectrics," The Journal of Physical Chemistry Letters **5**, 3677–3687 (2014) doi: 10.1021/jz501831q.

[27]Q. Chen and Q. Wang, "The effective electromechanical coupling coefficient of piezoelectric thin-film resonators," Applied Physics Letters **86**, 022904 (2005) doi: 10.1063/1.1850615.

[28]D. Royer and V. Kmetik, "Measurement of piezoelectric constants using an optical heterodyne interferometer," Electronics Letters **28**, 1828–1830 (1992) doi: 10.1049/el:19921166.